P(CL-b-PLLA) DIBLOCK COPOLYMERS GRAFTING ONTO CELLULOSIC NANOCRYSTALS
--Manuscript Draft--

Manuscript Number:	POBU-D-16-00490
Full Title:	P(CL-b-PLLA) DIBLOCK COPOLYMERS GRAFTING ONTO CELLULOSIC NANOCRYSTALS
Article Type:	Original Article
Section/Category:	Polymer Synthesis/Mechanism
Funding Information:	
Abstract:	Cellulose nanocrystals (CNCs) have attracted growing interest as a reinforcement agent in polymer matrices thanks to their biodegradability and excellent mechanical properties. However, due to the polar nature and strong interactions among them, CNCs form aggregates which are difficult to disperse in hydrophobic matrices. To improve CNCs' dispersion in apolar matrices, we have studied modifications via surface grafting with biodegradable polymers. In this work, CNCs were successfully modified with the P(CL-b-LLA) copolymer via a "grafting from" method. Firstly, the P(CL-b-LLA) copolymers (Mn molar mass of 6,190 Da and 10,500 Da) were synthesized by sequential copolymerization of E-caprolactone (CL) and L-lactide(LLA) using stannous octoate and 1-butanol as initiator and co-initiator, respectively. Then, the grafted CNCs, P(CL-b-LLA) g CNC, were obtained through the functionalization of copolymers with tolylene 2,4-diisocyanate and subsequent covalent linkage to CNCs' surface in dry toluene. Surface grafting was confirmed using Fourier transform infrared (FTIR), proton nuclear magnetic resonance (1H NMR), transmission electron microscopy (TEM), and thermogravimetry (TGA). TEM and TGA analyses indicated that the surface modification of the CNCs occurred to a greater extent with the use of the lower molecular weight copolymer. The resulting modified nanoparticles can find applications as filler and compatibilizer in the field of bionanocomposite materials.
Corresponding Author:	Valdir Mano, Ph.D. Universidade Federal de Sao Joao del-Rei São João del-Rei, Minas Gerais BRAZIL
Corresponding Author Secondary Information:	
Corresponding Author's Institution:	Universidade Federal de Sao Joao del-Rei
Corresponding Author's Secondary Institution:	
First Author:	Valdir Mano, Ph.D.
First Author Secondary Information:	
Order of Authors:	Valdir Mano, Ph.D.
	Stefano Chimenti
	Giacomo Ruggeri
	Fabiano Vargas Pereira
	Everton Luiz de Paula
Order of Authors Secondary Information:	
Author Comments:	São João del-Rei, Brazil, September, 05, 2016. Prof. K. Müllen Polymer Bulleton - Editor Dear Prof. Müllen

We are submitting the manuscript entitled "P(CL-b-PLLA) diblock copolymers grafting onto cellulosic nanocrystals" to be considered for publication as research paper in the Polymer Bulletin.

In this work, we described the modification of cellulose nanocrystals with P(CL-b-LLA) copolymer via a "grafting from" method. The grafted cellulose nanocrystals, P(CL-b-LLA)-g-CNC, were obtained through the functionalization of copolymers with tolylene 2,4-diisocyanate and subsequent covalent linkage to cellulose nanocrystals' surface in dry toluene. Surface grafting was confirmed by FTIR, 1H NMR, TEM and TGA. We believe that the results presented here show the possibility of controlling the grafting degree by varying the molecular weight of the copolymer.

In this way, we believe that this article is suitable for publication in Polymer Bulletin and can be of interest for those researchers concerned with renewable materials, biodegradable polymers, and bio-based nanocomposites.

All authors have seen and approved the submission of this manuscript.

With best regards,

Prof. Valdir Mano (corresponding author)
Departamento de Ciências Naturais
Universidade Federal de São João del-Rei
Praça Dom Helvécio, 74
CEP: 36301-160 - São João del-Rei, Brazil
mano@ufsj.edu.br

Suggested Reviewers:	
	Juan Pedro Bretas Roa, Ph.D. Professor, Universidade Federal dos Vales do Jequitinhonha e Mucuri juan.roa@ict.ufvjm.edu.br Dr. Roa develops his research in the polymer degradation area.
	Gilberto Siqueira, Ph.D. Empa Materials Science and Technology gilberto.siqueira@empa.ch Dr. Siqueira conducts research with cellusose nanocrystals.
	José Marconcini Empresa Brasileira de Pesquisa Agropecuaria jose.marconcini@embrapa.br Dr. Marconcini develops research on biomaterials.
	Rossana Thiré, Ph.D. Universidade Federal do Estado do Rio de Janeiro rossana@metalmat.ufrj.br Dr. Thiré develops studies with polymeric biomaterials.

1   **P(CL-*b*-PLLA) DIBLOCK COPOLYMERS GRAFTING ONTO CELLULOSIC NANOCRYSTALS**

2   **Valdir Mano[1]*, Stefano Chimenti[2], Giacomo Ruggeri[2], Fabiano Vargas Pereira[3], Everton Luiz de Paula[4]**

3

4   [1]Department of Natural Sciences, Federal University of São João del-Rei, Praça Dom Helvécio 74, 36301-160

5   São João del-Rei - MG, Brazil, mano@ufsj.edu.br

6   [2]Department of Chemistry and Industrial Chemistry, University of Pisa, Via Giuseppe Moruzzi 13, 56124 Pisa,

7   Italy

8   [3]Department of Chemistry, Federal University of Minas Gerais, Avenida Antônio Carlos 6627, 31270-901 Belo

9   Horizonte - MG, Brazil

10   [4]Institute of Science and Technology, Federal University of Vales do Jequitinhonha e Mucuri, Rodovia MGT

11   367- km 583, 39100-000 Diamantina - MG, Brazil

12

13   **Abstract** Cellulose nanocrystals (CNCs) have attracted growing interest as a reinforcement agent in polymer

14   matrices thanks to their biodegradability and excellent mechanical properties. However, due to the polar nature

15   and strong interactions among them, CNCs form aggregates which are difficult to disperse in hydrophobic

16   matrices. To improve CNCs' dispersion in apolar matrices, we have studied modifications via surface grafting

17   with biodegradable polymers. In this work, CNCs were successfully modified with the P(CL-*b*-LLA) copolymer

18   via a "grafting from" method. Firstly, the P(CL-*b*-LLA) copolymers (Mn molar mass of 6,190 Da and

19   10,500 Da) were synthesized by sequential copolymerization of ε-caprolactone (CL) and L-lactide (LLA) using

20   stannous octoate and 1-butanol as initiator and co-initiator, respectively. Then, the grafted CNCs,

21   P(CL-*b*-LLA)-*g*-CNC, were obtained through the functionalization of copolymers with tolylene-2,4-diisocyanate

22   and subsequent covalent linkage to CNCs' surface in dry toluene. Surface grafting was confirmed using Fourier

23   transform infrared (FTIR), proton nuclear magnetic resonance (^{1}H NMR), transmission electron microscopy

24   (TEM), and thermogravimetry (TGA). TEM and TGA analyses indicated that the surface modification of the

25   CNCs occurred to a greater extent with the use of the lower molecular weight copolymer. The resulting modified

26   nanoparticles can find applications as filler and compatibilizer in the field of bionanocomposite materials.

27

28   **Keywords** Cellulose nanocrystals; surface modification; P(CL-*b*-LLA) copolymer; bionanocomposite.

29

30

31   **Introduction**

32

33   Cellulose is one of the most abundant and naturally occurring polymers in the world which can be obtained from

34   numerous resources [1]. It is a carbohydrate formed by both crystalline and disordered amorphous domains.

35   Cellulose chains are stabilized laterally in the cell walls by hydrogen bonding between hydroxyl groups,

36   resulting in the formation of bundles of microfibrils. Carefully conducted acid treatment of microfibrils allows

37   the isolation of crystalline cellulose nanocrystals (CNC), also named cellulose nanowhiskers (CNW) [2]. These

38   highly crystalline rod-shaped nanomaterials, whose dimensions depend on the source of cellulose, present high

39   modulus (around 100 GPa) [3] and can be obtained from various sources such as natural fibers and sea animals

[4]. The extraction of cellulose nanocrystals from renewable sources has gained more attention in recent years due to their exceptional mechanical properties (high specific strength and modulus), large specific surface area, high aspect ratio (L/d, L being the length and d the diameter), environmental benefits and low cost [5].

The attraction for cellulose nanocrystals as nanofillers in polymer matrices, yielding CNC nanocomposites (also named bio-nanocomposites), has largely increased over the past decade, as indicated by the flourishing literature. CNCs offer many advantages such as high reactivity, renewability, biodegradability, and natural abundance. In addition, the unique combination of their impressive mechanical properties with their nanoscale dimensions and high aspect ratio gives them the qualities required for ideal filler agents used in polymer-based composites [6].

Despite its great potential as nanofiller, the hydrophilic nature of native cellulose generally limits the formation of CNC nanocomposites to water-soluble polymers; attractive forces lead to CNCs aggregation and poor cohesion with hydrophobic matrices [7]. Because of the incompatibility with the hydrophobic polymeric matrixes, it has been almost impossible to efficiently incorporate cellulose nanocrystals to most of the classical apolar polymers [8]. To overcome this major drawback, cellulose nanocrystals' surface chemical modification has been studied with the aim of improving their interfacial compatibility with a wider variety of polymer matrices. Efforts to enhance the compatibility are broadly documented in the literature including, among other examples, the use of surfactants [9,10], the acetylation of CNC surface using mixtures of acetic acid and anhydride [11], the acylation by drying aqueous emulsion [12], and superficial polymer grafting, which is achieved by two strategies: grafting "from" [6,13] and grafting "onto" [14,15]. In the "grafting from" approach, the polymer chains are formed by *in situ* surface-initiated polymerization from immobilized initiators on the substrate [16]. Habibi and co-workers [17] described the grafting of polycaprolactone onto the surface of CNCs via ring-opening polymerization (ROP) using stannous octoate [Sn(Oct)$_2$] as a grafting and polymerization agent. In the "grafting onto" approach, polymeric chains are linked onto the CNC surface via reactions involving hydroxyl groups and coupling agents. By this method, Labet and co-workers [14] described the successful modification of CNC with poly(tetrahydrofuran), poly(caprolactone), and poly(ethylene glycol)monobutyl ether using toluene 2,4-diisocyanate as a linking agent.

Our research group has been dedicated to studying CNC in different research fronts such as the production of CNC-grafted polymeric biodegradable matrices (e.g. PDLLA, cassava starch and chitosan) yielding bionanocomposites via casting solution [18,19] and the layer-by-layer technique and bionanocomposite synthesis through covalent linkage with chitosan via the "grafting onto" method. Keeping the track on this same line of study this present work describes the surface modification of CNC with the P(CL-*b*-LLA) copolymer via a "grafting from" method using tolylene-2,4-diisocyanate as a linking agent. This copolymer was chosen due to the intrinsic biodegradability of its constituents and because this grafting method broadens the possibilities of utilization of surface modified CNCs on the preparation of new bionanocomposites based on hydrophobic polymers such as PCL, PLLA and its copolymers.

Experimental

Materials

Eucalyptus wood pulp commercial samples were used as a source of CNCs. Sulfuric acid was purchased from Synth (São Paulo, Brazil). All other chemicals were acquired from Sigma Aldrich (St. Louis, USA): L-Lactide (98%) was dried under a vacuum for 5 h, at ambient temperature; ε-caprolactone (CL, 98%), 1-butanol (BuOH), and toluene were dried over calcium hydride for 24 h at room temperature, distilled under reduced pressure in a nitrogen atmosphere prior to use and stored under nitrogen and 4 Å molecular sieves; stannous octoate [$Sn(Oct)_2$, 95%], was used as received; N,N-dimethylformamide (DMF) and tolylene-2,4-diisocyanate (2,4-TDI, 95%) were distilled under reduced pressure in a nitrogen atmosphere and stored over 4 Å molecular sieves.

Extraction of cellulose nanocrystals

Cellulose nanocrystals were extracted from eucalyptus wood pulp through sulfuric acid hydrolysis according to the method previously described by de Paula et al [18]. For our purposes, CNCs aqueous dispersions were freeze-dried and kept in moisture-free environment.

Sequential synthesis of the P(CL-b-LLA) copolymers

P(CL-*b*-LLA) copolymers were synthesized via two-step sequential ring opening polymerization of ε−caprolactone and L-lactide in the presence of $Sn(Oct)_2$ (0.0798 g; 1.97 x 10^{-4} mol) and BuOH [BuOH/$Sn(Oct)_2$ = 2] as the initiating system to control the molar mass. As an example, the polymerization of CL (0,5 g) was carried out in 15 mL of dry toluene at 110 °C for 24 h, under a nitrogen atmosphere and reflux, producing the PCL prepolymer. Then, L-lactide (0,5 g) was further polymerized in the same reaction vessel for 24 h to achieve P(CL-*b*-LLA). The concentrations of monomers, $Sn(Oct)_2$ and BuOH were chosen so as to obtain an estimated molar mass in the range of 5 kDa. In all steps, scrupulous attention was paid to reagents' purity and apparatus' dryness, since even trace amounts of moisture or other hydroxyl-containing impurities can influence the molar mass of the final product. Characterization of the block copolymer was carried out by using FT-IR spectroscopy, ^{1}H nuclear magnetic resonance (^{1}H NMR), gel permeation chromatography (GPC), and differential scanning calorimetry (DSC).

Functionalization of the P(CL-b-LLA) copolymers with toluene 2,4-diisocyanate (2,4-TDI) and subsequent grafting on CNCs

In a typical reaction, 5 g of the P(CL-*b*-LLA) copolymer, Mn = 5 kD, which was synthesized as described in the previous paragraph, were added to 25 mL of anhydrous toluene in a two-neck reaction flask, previously dried under vacuum and heating. This mixture was kept under stirring until complete dissolution of the copolymer and then 2 μL of $Sn(Oct)_2$ and 120 μL of 2,4-TDI were added. A reflux condenser was adapted to the reaction flask and the system was kept in the temperature range of 80 to 90 °C under stirring and inert nitrogen atmosphere. After 24 h, a dispersion of CNCs in anhydrous toluene (0.25% by mass with respect to the copolymer) was added and the reaction was allowed to continue for another 7 days. To facilitate CNCs dispersion in toluene, the nanocrystals suspension was transferred from water to *tert*-butanol prior to use, which minimizes the aggregation

120 during the freeze drying process according to Petersson et al [20]. Finally, to improve nanocrystals' dispersion in

121 toluene the suspensions were exposed to three sonication intervals (UP400S, Hielscher Ultrasonics GmbH,

122 Germany) of 2 min each in ice bath. During the sonication cycles the suspensions were placed in an ice bath.

123 Reaction progress was monitored by FT-IR analysis. At the end of the reaction, the product, named

124 P(CL-*b*-LLA)-*g*-CNC, was recovered by precipitation in heptane, filtered off and subsequently dried under high

125 vacuum for 6 h. The purification procedure was performed twice. The characterization was carried out by using

126 FT-IR spectroscopy, transmission electron microscopy (TEM), differential scanning calorimetry (DSC), and

127 thermogavimetry (TGA).

128

129 *Characterizations*

130

131 ^{1}H NMR spectra were obtained using a Varian Gemini 300 MHz nuclear magnetic resonance spectrometer. All

132 measurements were carried out at 25 °C and deuterated chloroform (CDCl$_3$) was used as solvent.

133 Infrared spectra were recorded with a Perkin-Elmer Spectrum One FT-IR spectrophotometer interfaced

134 with the software Spectrum v.3.02 for data acquisition. Samples were analysed on transmission mode in KBr

135 windows as cast films from THF or CHCl$_3$, for solid samples, or directly as a liquid film from the crude reaction.

136 DSC measurements were performed with a Mettler DSC30 apparatus using 5 mg of sample specimen,

137 according to the following temperature program: from 30 °C to 250 °C at 10 °C min^{-1}; cooling from 250 °C

138 to -100 °C at 10 °C min^{-1}; isotherm for 3 min; and heating from -100 °C to 250 °C at 10 °C min^{-1}.

139 TGA were performed using a TGA Q500 thermogravimetric analyzer from Mettler with a heating ramp

140 of 20 °C min^{-1} under nitrogen flow (60 cm^3 min^{-1}) from room temperature to 600 °C. The samples were

141 previously dried in oven at 40 °C for 24 h.

142 Size exclusion chromatography (SEC) analyses were carried out with a Jasco instrumental setup

143 consisting of a PU-2089 Plus high pressure pump, RI 2031 Plus (refractive index) and UV-2077 Plus (UV)

144 detectors, and a Jasco CO-2063 Plus columm oven. Two PLgel 5 μm Mixed-D columns (Polymer Laboratories)

145 mounted in series with a guard column were used for elutions with organic solvents. The instrument was

146 interfaced with a Jasco ChromNav 1.12.01 software for data acquisition and processing. Sample concentration in

147 THF was in the 3-5 mg mL^{-1} range and injection volume was 20 μL. A DMF/LiBr (1 g L^{-1}) eluent solution

148 (30 °C; 1 mL min^{-1}; 6.1 MPa) and polystyrene standards (Polymer Laboartories) were used for all SEC analyses.

149 TEM images were obtained from a Tecnai G2-Spirit microscope (Netherlands, FEI) operating at 120

150 kV. For the TEM images, a drop of aqueous dispersions was placed onto a carbon-Formvar-coated copper grid

151 and subsequently stained with 2% uranyl acetate solution.

152

153

Results and discussions

154

155

Synthesis and characterization of the P(CL-b-PLLA) copolymers

156

157

158 The copolymers were synthesized according to Scheme 1. In this method, the polymerization of the LLA block

159 is initiated by the hydroxyl end groups of the PCL pre-polymers synthesized in the first step [21-24]. Kricheldorf

et al [25] reported that the transesterification does not occur in the polymerization of D,L-lactide catalyzed by

161 stannous octoate at temperatures below 120 °C. Thus, we chose to perform both reaction steps at 110 °C to avoid

162 transesterification. The PCL-OH pre-polymer was synthesized in a first step and, in the same reaction vessel, the

163 P(CL-*b*-LLA) copolymer was obtained by successive additions of the L-lactide monomer. By this route, the

164 P(CL-*b*-LLA) copolymer was prepared by ring-opening polymerization of successively added CL and LLA in

165 the presence of Sn(Oct)2 as initiator and 1-butanol (BuOH) as the co-initiator. Three copolymers with different

166 molecular weights, named CopB6, CopB12, and CopB24 were prepared by changing the molar ratio of CL and

167 LAA to $Sn(Oct)_2$, maintaining the ratio $BuOH/Sn(Oct)_2 = 2$, as showed in Table 1.

168

169 **Scheme 1** Sequential block copolymerization of CL and LLA

170

171 **Table 1 about here**

172

173 The primary evidence for the formation of the copolymers was provided by ^{1}H NMR. Fig. 1 shows the

174 NMR spectra of the PCL-OH prepolymer and the CopB6 copolymer. The signals of $–CH_2OH$, the methylene

175 protons of the hydroxyl end groups of the PCL prepolymers, at 3.6 ppm, disappeared and new signals that arise

176 from the copolymer's $-CH(CH_3)OH$ end group (detail in the Fig. 1b; methine proton F; $\delta = 4.32$ ppm) were

177 observed. This indicated that the PCL-OH reactive chains had initiated the polymerization of LLA. Copolymer

178 compositions were determined from the ^{1}H NMR spectra by taking the ratio of the peak areas corresponding to

179 the LLA methine protons at $\delta = 5.12$ ppm and the CL methylene protons at 1.36 ppm. The calculated

180 compositions (CL:LLA mol %) for CopB6 and CopB12 were 60:40 and 45:55, respectively.

181

182 **Fig. 1** ^{1}H NMR spectra of (a) PCL-OH prepolymer and (b) CopB6 (in detail the absorption of the terminal

183 methine group - proton F)

184

185 Furthermore, FT-IR analysis provided additional evidence for the formation of a block copolymer

186 instead of the random one. For CopB6, which is typical for the other compositions, two absorption peaks related

187 to the ester carbonyl groups, one at 1759 cm^{-1} due to the PLLA block and another at 1737 cm^{-1} belonging to the

188 PCL block, are observed in Fig. 2. In contrast, as reported by Qian et al [26], it should be observed only one

189 ester carbonyl absorption centered at 1756 cm^{-1} for a random copolymer.

190

191 **Fig. 2** FT-IR spectrum of the copolymer CopB6

192

193 In addition, the SEC (Fig. 3) results also indicated the successful initiation of LLA polymerization by

194 PCL-OH pre-polymer. Had not the PCL-OH pre-polymer initiated the polymerization, there should be two peaks

195 on the SEC curve belonging to the PCL and PLLA homopolymers. All of the copolymers gave similar unimodal

196 SEC molecular weight distributions, an example of which is shown in Fig. 3 for CopB6. The elution volumes are

197 smaller than that of PCL-OH, indicating that there is no pre-polymer in the final product.

198

199 **Fig. 3** SEC curves of the block copolymer CopB6 and the PCL-OH

The melting and crystallization behaviors of the block copolymers were investigated by DSC. The copolymer CopB12 exhibited two melting endothermic peaks (Tm) during heating and two crystallization exothermal peaks (Tc) during cooling. On the other hand, for CopB6 the crystallizations were observed only in the second heating run. Table 2 summarizes the main information obtained by DSC. The results indicated that both PCL and PLLA blocks crystallize and form two different crystal domains. In other words, the microphase separation took place in these block copolymers.

Table 2 about here

Functionalization of P(CL-b-LLA) copolymer with 2,4-TDI and grafting on CNCs

In order to graft the P(CL-*b*-LLA) copolymer onto the CNCs surface we used toluene 2,4-diisocyanate as linking agent as proposed by Labet et al [14]. The cellulose nanocrystals were functionalized by grafting the CopB6 (Mn 6 kDa) and CopB12 (Mn 12 kDa) copolymers to its surface, resulting in the modified CNCs named Bionano6 and Bionano12, respectively (Scheme 2).

Scheme 2 Functionalization of P(CL-*b*-LLA) and grafting on CNCs

Taking into account the average length of the extended chains, CopB6 and CopB12 grafting resulted in surface functionalization with an expected layer thickness ranging between 10 and 20 times the thickness of nanoparticles. These chain lengths were expected to be high enough to allow the formation of a continuous film by hot-pressing the functionalized CNCs [14]. On the other hand, long chains result in low concentration of urethane carbonyls compared to the carbonyls of the PCL and PLLA segments, which hampers its characterization by conventional methods such as FT-IR. In our studies, the surface functionalization of CNCs was characterized by observing the ^{1}H NMR absorptions of the benzene ring of 2,4-TDI between 7 and 7.2 ppm (Fig. 4). In addition and as expected, the FT-IR band at 2250 cm^{-1} corresponding to the isocyanate groups was not observed after 7 days of reaction time (Fig. 5).

Fig. 4 ^{1}H NMR spectrum of Bionano6 (expanded region related to the absorption of benzene protons)

Fig. 5 FT-IR spectrum of the Bionano6

Fig. 6 shows transmission electron micrographs of unmodified CNCs, Bionano6, and Bionano12. Using several TEM images, the mean values for the length (L) and diameter (D) of the unmodified rod-like nanocrystals were estimated to be 145 ± 25 nm and 6 ± 1.5 nm, respectively. In recently published studies, Dufresne [27] and Eichhorn [2] agreed that the morphology of nanocrystals plays a key role in the properties of nanocomposites, so it is important to ensure that CNCs' morphology has not been significantly altered because of chemical modification. Bionano12 TEM image (Fig. 6b) shows that the morphology of the individual CNCs did not change after grafting with CopB12. The nanocrystals maintained their elongated morphology with the

same length and aspect ratio as that of the unmodified CNCs; however, they kept the typical behavior of aggregate formation which is typical for the unmodified nanocrystals. Morphological changes were more noticeable in the aggregate for Bionano6 (Fig. 6c), in which the crystals appeared smaller in relation to the unmodified CNCs. On the other hand, formation of aggregates was avoided and the crystals were more disperse in the polymeric matrix. This behavior can be explained by the lower molar mass of CopB6, which led to a higher degree of grafting and, consequently, to a decrease in the hydrophilicity and strong surface interactions among the nanocrystals, improving their dispersion.

Fig. 6 TEM images of the unmodified CNCs (a), Bionano12 (b), and Bionano6 (c)

Many biomaterials suffer from inferior thermal properties when compared to inorganic fillers, especially when they are used as reinforcement for polymers melt processed at elevated temperatures. Therefore, thermal stability is a crucial factor and it is important that the grafting will not significantly change the copolymer thermal behavior. Thermogravimetric curves of P(CL-*b*-LLA), Bionano6, and Bionano12 are shown in Fig. 7. As reported by Rosa et al [28], for the CNCs, the thermal degradation occurs in a single step with Tmax at about 277 °C. The shoulder at 300 °C and the final residue correspond to remaining lignin which is not removed on the process of CNCs extraction. On the TGA curves of both Bionano6 and Bionano12 (Fig. 7.b), it was not possible to observe any event that could be attributed to the nanocrystals due to their low concentration (0.25% by mass with respect to the copolymer). On these curves we could also observe a degradation event due to the PLLA block, at a lower temperature, and another related to the PCL block, at a higher temperature. Also, the degradation profile was very similar to the starting copolymer (Fig. 7.a), indicating that the grafting process did not result in a decrease in thermal stability of the PLLA and PCL blocks. However, for the Bionano6, it is possible to notice a significant decrease on the degradation rate on the step relative to PLLA when compared to the initial P(CL-*b*-LLA) copolymer. If we consider the mechanism of synthesis, a reduction on the degradation rate by effect of the incorporation of nanocrystals is in agreement with the hypothesis of its grafting onto the end of the PLLA block. This effect would not be observed if the nanocrystals were agglomerates within the matrix. On the other hand, the progress of thermal degradation for Bionano12 didn´t show any significant differences from the starting copolymer so, and considering the results of TEM, it is not possible to conclude that the copolymer CopB12 was grafted onto the CNCs' surface.

Fig. 7 TGA curves of P(CL-*b*-LLA) (a) and Bionano6 and Bionano12 (b)

Conclusions

CNCs were grafted with the P(CL-*b*-LLA) copolymers, yielding the P(CL-*b*-LLA)-*g*-CNC functionalized nanocrystals. The first part of this work was dedicated to the sequential copolymerization of CL and LLA using Sn(Oct)$_2$ and BuOH as initiator and co-initiator, respectively. The P(CL-*b*-LLA) copolymers with Mn molar mass of 6,190 Da (CopB6) and 10,500 Da (CopB12) were fully characterized by ^{1}H NMR, FT-IR, GPC, and DSC. On the second part, the grafted CNCs were obtained through the functionalization of CopB6 and CopB12

copolymers with 2,4-TDI and subsequent covalent linkage to cellulose nanocrystals' surface in dry toluene, yielding the grafted cellulose nanocrystals P(CL-*b*-LLA)-*g*-CNC, named Bionano6 and Bionano12. The grafting efficiency was evidenced by characterization with ^{1}H NMR, FT-IR, TEM, and TGA. TEM analysis indicated that the surface modification of the CNCs occurred to a greater extent with the use of the lower molecular weight copolymer (CopB6), which led to a higher grafting degree and consequent decrease in hydrophilicity and aggregation. By TGA results, we had an another evidence that the grafting was more effective for Bionano6 than for Bionano12, indicating that the control of the molecular weight is essential for the successful modification of CNCs. The approach used in this work proved to be successful towards CNC grafting and can be extended to other polymers and copolymers to produce functionalized CNCs with new properties and potential applications.

Acknowledgments

References

1. Klemm D, Heublein B, Fink HP, Bohn A (2005) Cellulose: Fascinating biopolymer and sustainable raw material. Angew Chem Int Edit 44:3358-3393. doi:10.1002/anie.200460587.

2. Eichhorn SJ (2011) Cellulose nanowhiskers: promising materials for advanced applications. Soft Matter 7:303-315. doi:10.1039/c0sm00142b.

3. Rusli R, Eichhorn SJ (2008) Determination of the stiffness of cellulose nanowhiskers and the fiber-matrix interface in a nanocomposite using Raman spectroscopy. Appl Phys Lett 93:033111-1.3. doi:10.1063/1.2963491.

4. Samir ASA, Alloin F, Dufresne A (2005) Review of recent research into cellulosic whiskers, their properties and their application in nanocomposite field. Biomacromolecules 6:612-626. doi:10.1021/bm0493685.

5. Medeiros ES, Mattoso LHC, Bernardes-Filho R, Wood DF, Orts WJ (2008) Self-assembled films of cellulose nanofibrils and poly(o-ethoxyaniline). Colloid Polym Sci 286: 1265-1272. doi:10.1007/s00396-008-1887-x.

6. Goffin A-L, Raquez JM, Duquesne E, Siqueira G, Habibi Y, Dufresne A, Dubois P (2011) From interfacial ring-opening polymerization to melt processing of cellulose nanowhisker-filled polylactide-based nanocomposites. Biomacromolecules 12:2456-2465. doi:10.1021/bm200581h.

7. Braun B, Dorgan JR (2009) Single-step method for the isolation and surface functionalization of cellulosic nanowhiskers. Biomacromolecules 10:334-341. doi:10.1021/bm8011117.

8. Ljungberg N, Bonini C, Bortolussi F, Boisson C, Heux L, Cavaillé JY (2005) New nanocomposite materials reinforced with cellulose whiskers in atactic polypropylene: Effect of surface and dispersion characteristics. Biomacromolecules 6:2732-2739. doi:10.1021/bm050222v.

9. Ljungberg N, Cavaillé JY, Heux L (2006) Nanocomposites of isotactic polypropylene reinforced with rod-like cellulose whiskers. Polymer (Guildf) 47:6285-6292. doi:10.1016/j.polymer.2006.07.013.

319   10. Heux L, Chauve G, Bonini C (2000) Nonflocculating and chiral-nematic self-ordering of cellulose

320   microcrystals suspensions in nonpolar solvents. Langmuir 16:8210-8212. doi:10.1021/la9913957.

321   11. Sassi JF, Chanzy H (1995) Ultrastructural aspects of the acetylation of cellulose. Cellulose 2:111-127.

322   doi:10.1007/BF00816384.

323   12. Yuan H, Nishiyama Y, Wada M, Kuga S. (2006) Surface acylation of cellulose whiskers by drying aqueous

324   emulsion. Biomacromolecules 7:696-700. doi:10.1021/bm050828j.

325   13. Goffin A-L, Habibi Y, Raquez JM, Dubois P (2012) Polyester-grafted cellulose nanowhiskers: A new

326   approach for tuning the microstructure of immiscible polyester blends. ACS Appl Mater Interfaces 4:3364-3371.

327   doi:10.1021/am3008196.

328   14. Labet M, Thielemans W, Dufresne A (2007) Polymer grafting onto starch nanocrystals. Biomacromolecules

329   8:2916-2927. doi:10.1021/bm700468f.

330   15. Thielemans W, Belgacem MN, Dufresne A (2006) Starch nanocrystals with large chain surface

331   modifications. Langmuir 22:4804-4810. doi:10.1021/la053394m.

332   16. Habibi Y, Lucia LA, Rojas OJ (2010) Cellulose nanocrystals: chemistry, self-assembly, and applications.

333   Chem Rev 110: 3479-3500. doi:10.1021/cr900339w.

334   17. Habibi Y, Goffin A-L, Schiltz N, Duquesne E, Dubois P, Dufresne A (2008) Bionanocomposites based on

335   poly(ε-caprolactone)-grafted cellulose nanocrystals by ring-opening polymerization. J Mater Chem 18:5002-

336   5010. doi:10.1039/b809212e.

337   18. de Paula EL, Mano V, Pereira FV (2011) Influence of cellulose nanowhiskers on the hydrolytic degradation

338   behavior of poly(d,l-lactide). Polym Degrad Stabil 96:1631-1638. doi:10.1016/j.polymdegradstab.2011.06.006.

339   19. da Silva JBA, Pereira FV, Druzian JI (2012) Cassava starch-based films plasticized with sucrose and inverted

340   sugar and reinforced with cellulose nanocrystals. J Food Sci 77:14-19. doi:10.1111/j.1750-3841.2012.02710.x.

341   20. Petersson L, Kvien I, Oksman K (2007) Structure and thermal properties of poly(lactic acid)/cellulose

342   whiskers nanocomposite materials. Compos Sci Technol 67:2535-2544. doi:10.1016/j.compscitech.2006.12.012.

343   21. in't Veld PJA., Velner EM, Van De Witte P, Hamhuis J, Dijkstra PJ, Feijen J (1997) Melt block

344   copolymerization of ε-caprolactone and L-lactide. J Polym Sci Pol Chem 35:219-226. doi:10.1002/(SICI)1099-

345   0518(19970130)35:2<219::AID-POLA3>3.0.CO;2-N.

346   22. Kikkawa Y, Kurokawa K, Kimura R, Takahashi M, Kanesato M, Abe H (2010) Solvent-induced

347   morphological diversification in poly(L-lactide-b-ε-caprolactone) block copolymer thin films. Polym Degrad

348   Stabil 95:1414-1420. doi:10.1016/j.polymdegradstab.2010.01.005.

349   23. Kim JK, Park D-J, Lee M-S, Ihn KJ (2001) Synthesis and crystallization behavior of poly(L-lactide) -block-

350   poly(ε-caprolactone) copolymer. Polymer (Guildf) 42:7429-7441.

351   24. Kong JF, Lipik V, Abadie MJ, Deen GR, Venkatraman SS (2012) Biodegradable elastomers based on ABA

352   triblocks: Influence of end-block crystallinity on elastomeric character. Polym Int 61:43-50.

353   doi:10.1002/pi.3130.

354   25. Kricheldorf HR, Boettcher C, Tönnes K-U (1992) Polylactones: 23. Polymerization of racemic and meso

355   D,L-lactide with various organotin catalysts - stereochemical aspects. Polymer (Guildf) 33:2817-2824.

356   doi:10.1016/0032-3861(92)90459-A.

357   26. Qian H, Bei J, Wang S (2000) Synthesis, characterization and degradation of ABA block copolymer of L-

358   lactide and ε-caprolactone. Polym Degrad Stabil 68:423-429. doi:10.1016/S0141-3910(00)00031-8.

359   27. Dufresne A (2010) Processing of polymer nanocomposites reinforced with polysaccharide nanocrystals.

360   Molecules 15:4111-4128. doi:10.3390/molecules15064111.

361   28. Rosa MF, Medeiros ES, Malmonge JA, Gregorski KS, Wood DF, Mattoso LHC, Glenn G, Orts WJ, Imam

362   SH (2010) Cellulose nanowhiskers from coconut husk fibers: Effect of preparation conditions on their thermal

363   and morphological behavior. Carbohyd Polym 81:83-92. doi:10.1016/j.carbpol.2010.01.059.

364   29. Ren J, Zhang Z, Feng Y, Li J, Yuan W (2010) Synthesis of star-shaped poly(e-caprolactone)-b-poly(L-

365   lactide) copolymers: from star architectures to crystalline morphologies. J Appl Polym Sci 118:2650-2658.

366   doi:10.1002/app.32590.

367

368   **FIGURE CAPTIONS**

369

370   **Scheme 1** Sequential block copolymerization of CL and LLA

371

372   **Scheme 2** Functionalization of P(CL-*b*-LLA) and grafting on CNCs

373

374   **Fig. 1** ^{1}H NMR spectra of (a) PCL-OH prepolymer and (b) CopB6 (in detail the absorption of the terminal

375   methine group - proton F)

376

377   **Fig. 2** FT-IR spectrum of the copolymer CopB6

378

379   **Fig. 3** SEC curves of the block copolymer CopB6 and the PCL-OH

380

381   **Fig. 4** ^{1}H NMR spectrum of Bionano6 (expanded region related to the absorption of benzene protons)

382

383   **Fig. 5** FT-IR spectrum of the Bionano6

384

385   **Fig. 6** TEM images of the unmodified CNCs (a), Bionano12 (b), and Bionano6 (c)

386

387   **Fig. 7** TGA curves of P(CL-*b*-LLA) (a) and Bionano6 and Bionano12 (b)

388

Table 1 Sequential copolymerization of CL and LLA in dry toluene at 110 °C using $Sn(Oct)_2$ and BuOH as initiator and co-initiator, respectively. The molar ratio $BuOH/Sn(Oct)_2$ was kept constant and equal to 2

Sample[a]	LLA (mmol)	CL (mmol)	$Sn(Oct)_2$ (mmol)	BuOH (mmol)	$Mn_{exp.}$[b] (Da)	Mn_{GPC}[c] (Da)	PD (Mw/Mn)
CopB6	151	187	7.19	14.4	5,988	6,190	1.2
CopB12	146	187	3.47	6.95	12,204	10,500	1.3
CopB24	7.0	8.76	0.0841	0.168	23,808	14,900	1.5

[a] The abbreviations CopB6, CopB12 and CopB24 mean block copolymers *P(CL-b-LLA)* with molecular weights expected of 6, 12 and 24 kDa, respectively.
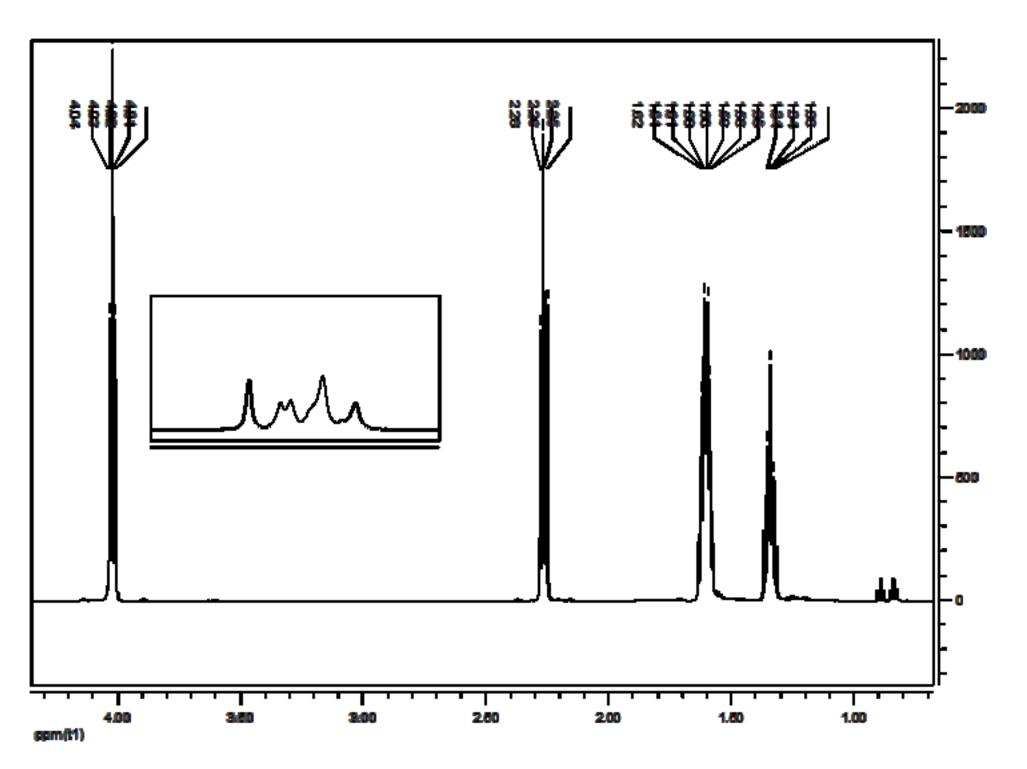[b] Expected number-average molecular weights were calculated considering 100% conversion and monomers/$Sn(Oct)_2$ ratio.
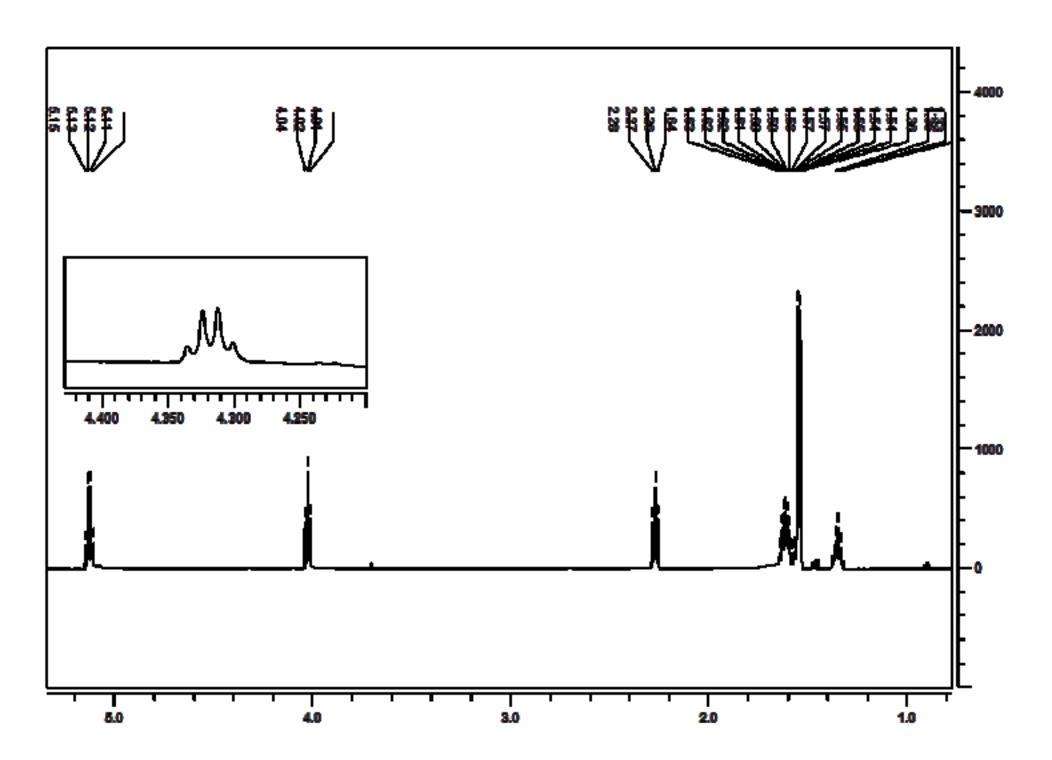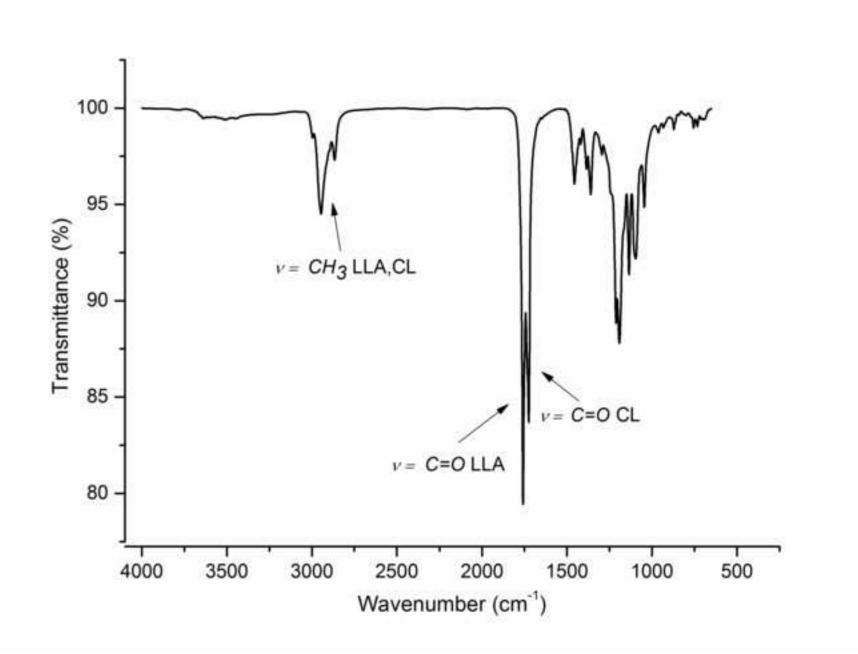[c] Number-average molecular weights determined by GPC measurements using the universal calibration technique.

Table 2 Melting and crystallization behaviors of CopB6 and CopB12 block copolymers

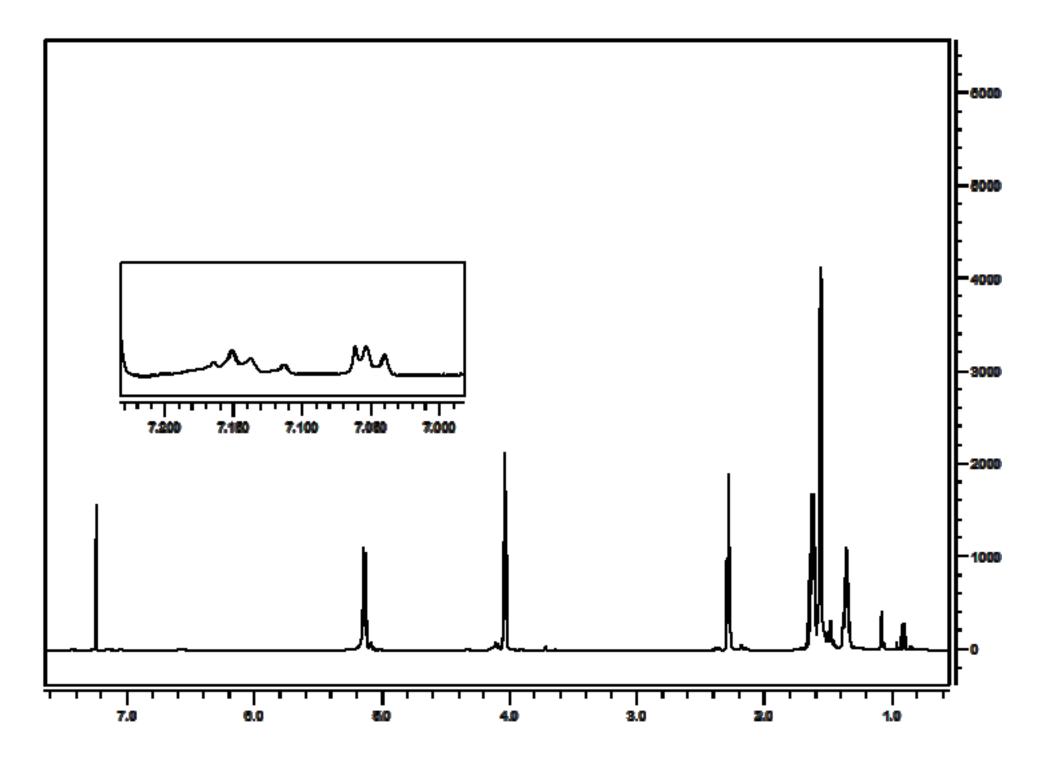| Co-polymer	$T_{g,PCL}$ (°C)	$T_{g,PLLA}{}^a$ (°C)	$T_{m,PCL}$ (°C)	$T_{m,PLLA}$ (°C)	$\Delta H_{m,PCL}$ (J g^{-1})	$\Delta H_{m,PLLA}$ (J g^{-1})	X_c (%)^b	
							$X_{c,PCL}$	$X_{c,PLLA}$
CopB6	-70	87	43	120	16	7	11.8	7.5
CopB12	-69	---	49	145	12	25	8.8	26.7

[b] It was not possible to determine the Tg of CopB12.

[b] X_c = degree of crystallinity = $\Delta H_m / \Delta H^o m$; $\Delta H^o m;_{PCL}$ is 136.1 J g^{-1}; $\Delta H^o m;_{PLLA}$ is 93.6 J g^{-1} (Ren et al. 2010).
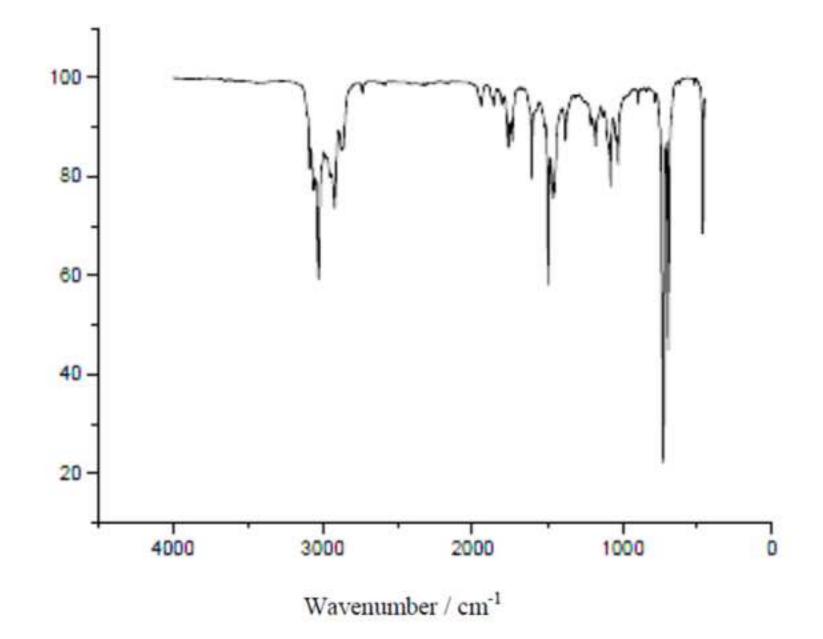
200 nm

100 nm

100 nm

$T_{max\ PLLA} = 256\ °C$

$T_{max\ PLLA} = 278\ °C$

$T_{max\ PCL} = 327\ °C$

$T_{max\ PCL} = 340\ °C$

b-
—— Bionano6
······ Bionano12

ε-caprolactone   butan-1-ol   PCL-OH

PCL-OH +   L-lactide   P(CL-δ-LLA)